Applied Catalysis B: Environmental 342 (2024) 123370

Contents lists available at ScienceDirect

Applied Catalysis B: Environmental

journal homepage: www.elsevier.com/locate/apcatb

Conversion of methane to methanol over Cu-MAZ (zeolite omega): An oxygen-free process using H_2O and CO_2 as oxidants

Tássia Caroline.P. Pereira [a], Jussara V.R. Vieira [a], Carlos H.F. da Cunha [a], Stefanie C.M. Mizuno [a], Yasmin O. Carvalho [a], Thiago Faheina [a], Monize Picinini [a], Asdrubal L. Blanco [b], Ana C.M. Tello [a], Ernesto A. Urquieta-Gonzalez [a], Alejandro Lopez-Castillo [b], Alice M. de Lima [a], João Batista O. dos Santos [a], José Maria C. Bueno [a,*]

[a] Department of Chemical Engineering, Federal University of São Carlos, P.O. Box 676, 13565-905 São Carlos, SP, Brazil
[b] Department of Chemistry, Federal University of São Carlos, P.O. Box 676, 13565-905, São Carlos, SP, Brazil

A B S T R A C T

Strong oxidants have been reported to be required in the catalytic oxidation of CH_4 to methanol in cyclic processes employing CuO-zeolites. Here, using Cu-exchanged zeolite omega (Cu-MAZ), it was demonstrated that O_2 could be replaced by CO_2, enabling the development of a new process. CuO-MAZ thermally treated in Ar, O_2, or CO_2 was investigated using *in situ* DRS-UV-Vis analysis and spectra calculated using density functional theory. The active species were characterized at different temperatures of reaction with CH_4. The species of the type Z_n-$[Cu_xO_y]^{n+}$ and main species Z-$[CuOH\text{-}HOCu]^{2+}$-Z were formed on Cu-MAZ. After the reaction with CH_4, the Cu^+ formed from Z_n-Cu_xO_y could be reoxidized with CO_2, while the Cu^+ formed from Z-CuOH-HOCu-Z was only reoxidized with H_2O, and not with CO_2. After reoxidation with H_2O, the activity of the material was fully restored by thermal treatment in O_2 or CO_2. The highest CH_3OH yield was achieved using CO_2.

1. Introduction

Access to the large global reserves of natural gas is generally associated with the extraction of crude oil, but the costs of compression and transport of the gas are prohibitive. At the same time, the direct emission of methane into the atmosphere (or its burning) results in serious environmental impacts. Hence, there is great interest in the conversion of methane into products that have higher added value, such as methanol, in compact plants [1]. Currently, in industry, this conversion is performed according to a two-step process [2]. The first step is the reforming of methane to produce synthesis gas (CO and H_2), which is highly endothermic and requires high temperatures. The second step is the formation of methanol at around 300 °C, under high pressure. Both steps have kinetic and thermodynamic constraints, requiring the use of large reactors [2–5]. In order to overcome these constraints, the direct selective oxidation of CH_4 to methanol can be performed using a process known as chemical looping. One of the most promising materials for this process is CuO-zeolite [3]. The reaction involves at least three steps: i) oxidation of methane to methanol by CuO clusters, with the methanol remaining adsorbed on the material; ii) extraction of methanol using H_2O vapor; and iii) reactivation of the material by thermal treatment using an oxidant such as O_2 or N_2O [3,6,7].

In the chemical looping process, methane is oxidized by Cu^{2+} clusters in zeolites, at temperatures of around 250 °C, forming methanol and Cu^+. The adsorbed methanol can then be desorbed with H_2O vapor [6]. In this step, Cu^+ is oxidized to Cu^{2+} by the action of H_2O, but the hydroxides formed have low activity, requiring reactivation at high temperatures. On the other hand, the active clusters in zeolites FAU, MFI, MOR, and CHA autoreduce when heated in an inert atmosphere, with the capacity for autoreduction depending on the nature of the zeolite, copper load, and temperature [6,8]. Hence, the reactivation requires the presence of an oxidant, such as O_2 or N_2O, to maintain the Cu^{2+} as the active species [3,7].

At low temperature (250 °C), CuO-MAZ provides a high methanol yield, when compared to a series of Cu-zeolite catalysts with different structures [9], with values of around 150 and 200 μmol of CH_3OH per gram of zeolite, at 1 and 30 bar, respectively [10]. Knorpp et al. [11] showed the existence of three possible sites for copper in the zeolite omega structure: (1) in the six-member ring (6-MR), and (2 and 3) in the 8-MR ring of the gmelinite (GME) cavity. The Cu^{2+} ions in (1) coordinate four oxygen atoms of the structure in the plane of the 6-MR ring, while the Cu^{2+} ions in (2) and (3) coordinate the structural oxygen atoms and a

* Corresponding author.
E-mail address: jmcb@ufscar.br (J.M.C. Bueno).

https://doi.org/10.1016/j.apcatb.2023.123370
Received 19 July 2023; Received in revised form 4 October 2023; Accepted 6 October 2023
Available online 6 October 2023

non-structural oxygen atom. The copper exchanged in the 6-MR rings was considered non-reactive, since it remained unaltered as Cu^{2+} in the reaction step. In the 8-MR rings of the GME cavities, Cu^{+} formed after the reaction was identified as the active species in the partial oxidation reaction of methane to methanol on Cu-MAZ. The copper ions in (2) and (3) form CuOH-HOCu dimers that present high activity for the partial oxidation of CH_4 [11], according to Reaction [1].

$$Z\text{-}CuOH\text{-}HOCu\text{-}Z + CH_4 \rightarrow CH_3OH + H_2O + 2Z\text{-}Cu^{+} \quad (1)$$

Although the chemical looping approach can provide high selectivity, economic analysis indicates that higher productivity is required than has so far been achieved [12], for which it would be necessary to increase the activity of the Cu-zeolite and decrease the cycle time. Increasing the CH_4 pressure above 15 bar has been found to have a positive effect in terms of increased activity [9,10,13], but without achieving sufficient productivity for the process to be economically viable.

Considering reduction of the cycle time, in addition to accelerating the reaction, mainly by the effect of temperature, the reactants employed should ideally also provide greater process safety, according to established safety principles [14,15]. This is especially critical when addressing potential explosion risks associated with methane and oxygen (O_2) mixtures. The chosen reactants should facilitate the rapid exchange of materials at each stage of the cycle and enable precise modulation of the reactor feed composition. This can be achieved by substituting oxygen with a mild oxidant, such as CO_2 [16,17]. Using CO_2, the time taken to remove the oxidizer should be faster, shortening the cycle time. Furthermore, the use of CO_2 increases the overall activity of the catalyst. It should be noted that this is the first time that CO_2 has been employed in the catalytic oxidation of CH_4 to methanol in cyclic processes with CuO-zeolite.

The aim of this work was to contribute to further development of the chemical looping process, demonstrating that CO_2 can substitute O_2 in the process. Although Cu-MAZ presents well-characterized main active sites of the type CuOH-HOCu our results show that the CuOH-HOCu species exhibits high thermal stability and resistance to auto reduction at the reactivation temperature, which would dispense the presence of oxidant. However, the species with oxide-like structure Zn-Cu(x > 3)Oy are self-reduced upon reactivation and require the presence of CO_2 to remain the species oxidized and active. Understanding the effect of CO_2 in terms of different active species that could be formed in applied CuO-zeolite treatments is crucial for the development of a new process for oxidation of methane to methanol using CO_2. The use of CO_2 allowed safe dynamic modulation of the CH_4, H_2O, and CO_2 reactants in the reactor feed.

2. MATERIAL: Synthesis and characterization

Na-zeolite omega (MAZ, SiAl = 2.7) was used as the matrix for preparation of all the Cu-zeolite omega (Cu-MAZ) materials investigated in this work. MAZ and Cu-MAZ (obtained by Cu exchange) were synthesized according to the procedure described in the Supporting Information (SI). DRX analysis indicated that the parent MAZ zeolite presented high crystallinity (Fig. S1), and NMR analysis showed absence of extra-framework Al (Fig. S2). The SEM results for the synthesized MAZ zeolite showed uniformly assembled nano-rod morphology, with aggregates of parallel rods (Fig. S3). These nano-rods had widths in the range from around 200–500 nm and lengths in the range from around 2–4 μm. Increasing the copper amount from 1 to 2 did not substantially alter the morphology. However, randomly arranged nano-rods were observed when the higher copper level was used. Despite this morphological change, no significant changes in the diffraction patterns were observed with increasing copper content. A small reduction could be seen in the intensity of the (110) peak at 2θ of around 10° [13]. Table 1 summarizes the composition of a series of copper-exchanged MAZ samples analyzed using ICP-OES, labeled *x*CuyMAZ, where *x* is the number of successive ions exchanged and *y* is the Al/Si ratio.

Table 1
Results of elemental analyses by ICP-OES of Cu-MAZ with different exchanged Cu^{2+} contents.

Sample	Cu wt%	Cu/Al
1Cu2.7MAZ	3.2	0.15
2Cu2.7MAZ	5.5	0.23
3Cu2.7MAZ	6.2	0.27

The results of chemical analysis by ICP-OES showed that the synthesized zeolite omega had a Si/Al ratio of 2.7 and a copper content that depended on the number of ionic exchanges applied to the catalyst. The Cu/Al ratio increased with successive ionic exchanges, but remained below 0.5, the maximum achievable Cu/Al ratio.

Analysis using X-ray diffraction (XRD) indicated formation of the zeolite omega structure (Fig. S1), which remained stable after successive ion exchange procedures, with no copper oxide diffraction peak detected. The ^{27}Al MAS NMR spectra (Fig. S2) showed the presence of two types of tetrahedral sites that were crystallographically non-equivalent, denoted T1 and T2 [18,19], with signals at around 60 and 55 ppm [20]. The ^{27}Al NMR spectrum is similar for omega zeolites with different morphology [13]. Using Rietveld refinement, Knorpp et al. [11] showed the presence of two copper sites in the 8-MR GME cavity. Exploratory anomalous X-ray diffraction (AXPD) analysis showed that these two copper sites could interact with each other across the narrow 8-member ring channel. However, there was a different interaction of copper in the 6-member rings.

Fig. S3 shows the zeolite morphology, consisting of interconnected rods forming bundles with width and length of approximately 2 and 4 μm, respectively. The samples presented well-defined morphology, indicating that they were highly crystalline, as also observed in the X-ray diffractograms. It was previously reported by Knorpp et al. [13] that MAZ with long bundle rods presented superior activity in the methane to methanol conversion reaction, when compared to other morphologies, which could be explained by higher thermal stability and faster reactant diffusion.

The activity of copper-exchanged zeolite depends on the occupation of Cu in the unit cell [11], with the ease of occupation depending on the zeolite morphology, since the latter influences several aspects of the material, such as diffusion limitation and pore blockage [13]. Therefore, it can be deduced that the rod-like morphology of zeolite omega facilitates copper occupation in the 8-MR GME cavity, so that this material is more active than zeolite omega with morphology consisting of small spherulitic aggregates, where copper occupation probably occurs in the 6-MR cavities of the structure, making this copper inactive [11,13].

3. Results: activity, *in situ and calculated* UV-Vis characterization

Comparison was made of samples obtained using O_2 or CO_2 in the **activation step** of copper-exchanged MAZ samples before use in

Table 2
Catalytic results for Cu2.7MAZ, varying the catalyst copper content and the oxidizing gas in the activation step. Activation step was at 450 °C and the reaction was at 250 °C and 1 bar.

Run	Catalyst	Oxidant gas	Micromol CH_3OH/g zeolite	Mol CH_3OH/ mol Cu
1	1Cu2.7MAZ	O_2	82	0.165
2		CO_2	94	0.190
3	2Cu2.7MAZ	O_2	103	0.119
4		CO_2	111	0.127
5	3Cu2.7MAZ	O_2	132	0.136
6		CO_2	163	0.167

catalytic cycle. Table 2 shows the effect of substituting O_2 by CO_2 as oxidant on the activity for methanol formation, using a series of samples prepared from Cu-MAZ with different Cu contents. Table S2 shows the influence of activation and reaction times on the methanol yield. Samples were treated according to the step-by-step procedures shown in the Supplementary Material, with sample activation at 450 ºC and reaction at 250 ºC with methane at 1 bar. The results (Table S2) reflect the general behavior observed, with high sensitivity to reaction time for the samples activated with O_2. The longer reaction time could be indicative of lower accessibility of CH_4 to the active sites for the samples activated with O_2, compared to activation with CO_2. The yield of methanol per mass of zeolite (g CH_3OH/g zeolite) increased with the copper content (Table 2). However, the yields per mol of Cu suggested that the occupation of Cu on the sites was similar for the Cu2.7MAZ samples. Interestingly, the methanol yield increased slightly when the catalyst was activated with CO_2 instead of O_2. These results suggested an increase of active species for methanol formation using Cu2.7MAZ, when activation was performed with CO_2.

Table 3 shows the methanol yields obtained with reuse of the 1Cu2.7MAZ and 2Cu2.7MAZ catalysts reactivated in second cycle with CO_2, with the methanol produced in the first cycle extracted online with water vapor at 250 ºC. The results indicated that activity were restored after methanol extraction and the samples reactivated with CO_2. Considering the previous literature results, the following conclusions could be drawn: I) The Z-CuOH species formed in Cu-MAZ become active when in 8-member rings of adjacent GME cavities, interacting to form paired copper monohydroxide monomer species (Z-CuOH.HOCu-Z). This interaction facilitated the two-electron redox mechanism for conversion of methane to methanol [11,21]; II) Cu_xO_y cluster species could autoreduce when heated in an inert gas, with the reduction temperature depending on the Cu load and the zeolite structure [8]; III) Experimental and theoretical works indicate that the sample treatments occurred as stepwise procedures, with the reoxidation of Cu^+ by H_2O occurring in the methanol extraction step [5,22,23]. From these results, the predominant Z-CuOH.HOCu-Z active species in the Cu-MAZ samples were reduced by methane and were then reactivated by H_2O vapor during methanol extraction. However, these results make it evident that the effect of CO_2 on the reactivation step is not still understood.

According to previous studies, the process of autoreduction of Z-CuOH species in MFI, MOR, and FAU zeolites can be represented by Scheme 1, involving the initial dehydration of neighboring Z-CuOH species, followed by autoreduction and elimination of O_2 [8,24,25].

Considering this previous work, the same methodology was used to study the CO_2 activation over $MAZ[Cu_2^+]^{2+}$ (see Model Systems and Theoretical Methods in the SI), for the first step of Scheme 1, namely dehydration of the Z-CuOH.HOCu-Z species in MAZ. A transition state of 220 kJ.mol^{-1} was obtained, disfavoring the autoreduction of CuOH-MAZ This autoreduction did not occur for the Cu-MAZ heated in CO_2, with these samples being slightly higher active, compared to the samples treated in O_2 (Table 2).

Further elucidation of the effect of CO_2 in catalyst activation was obtained by performing reaction cycles under isothermal conditions, at different temperatures. Activation with CO_2 and reaction with CH_4 employed the same temperature and 1 bar pressure. The catalyst was activated for 60 min in CO_2 and the reaction with CH_4 was continued for 30 min. The results are shown in Fig. 1.

Table 3
Catalyst recycling results using CO_2 for catalyst activation and reactivation.*.

Run	Catalyst	Number of cycles	Micromol CH_3OH/g zeolite	Mol CH_3OH/ mol Cu
2	1Cu2.7MAZ	1	94	0.190
7		2	76	0.152
4	2Cu2.7MAZ	1	111	0.127
8		2	109	0.126
10		3	116	0.132
11		4	118	0.135

* Extraction after the first cycle was performed online using water vapor. Methanol extraction after the second reaction cycle was performed offline. The catalysts were previously calcined in a flow of synthetic air at 500 ºC.

The yield in the isothermal process at 250 ºC was 13 μmol CH_3OH/g zeolite, while a maximum yield of 55 μmol CH_3OH/g zeolite was obtained at 350 ºC. For the non-isothermal process with the catalyst activated at 450 ºC, the yield at 250 ºC was 94 μmol CH_3OH/g zeolite. Despite the discovery that the catalysts could be activated by CO_2, instead of O_2, with the ability to perform the direct oxidation of CH_4 to methanol in an isothermal process at temperatures above 350 ºC, there was an abrupt decrease of the yield, suggesting methanol desorption associated with total methane oxidation. Hence, 350 ºC was a limiting temperature for catalyst activation. Comparison of the methanol yields obtained in isothermal cycles (Fig. 1) and non-isothermal cycles (Table 2, Run 2), at the same reaction temperature, showed that a lower methanol yield was obtained in the isothermal process, indicating the need to activate the sample at high temperature (450 ºC). Previous studies using Cu-MOR showed that the adsorption of water on Cu-MOR resulted in partial blocking of the active sites [6], which was reversible and could be resolved by dehydration at high temperature in O_2 and similar results were obtained now with CO_2.

The structures of the active species in the samples and the species reactivated by CO_2 were investigated using *in situ* DRS UV-Vis analyses. It should be noted that the procedure adopted enabled extraction of the spectra only of the active species, which were reduced by CH_4. The structures of the active species were identified from calculated spectra obtained using density DFT. Fig. 2 shows the calculated spectra for species of the types Z-CuOH.HOCu-Z, Z-Cu_3O_3-Z, and Z-Cu-O-Cu-Z (where Z is the framework of the MAZ zeolite) in the Cu-MAZ structure.

Fig. 2(a) shows the main bands for the paired copper monohydroxide monomers (Z-CuOH.HOCu-Z) at 36,000 and 41,600 cm^{-1}. Fig. 2(b) shows the bands for the Z-Cu_3O_3-Z trimer at 30,000 and 38,000 cm^{-1}. These results agreed with previous studies showing that species such as $CuOH^+$ present broad ligand-to-metal charge transfer (O→Cu) bands with maxima at around 36,000 and 41,600 cm^{-1} [26,27], while trinuclear type species (Z-Cu_3O_3-Z) present bands at around 30,000 and 38,000 cm^{-1}[25,28].

Fig. 3 shows the spectra for the 2Cu2.7MAZ sample (5.5 wt% Cu) thermally treated in an O_2 or CO_2 atmosphere at 450 ºC for 1 h. The spectra showed a broad ligand-to-metal charge transfer band with maximum at 41,200 cm^{-1}. Comparison with the calculated spectra obtained by DFT (Fig. 2) suggested the predominant presence of $CuOH^+$, with paired copper monomers type structure (Z-CuOH.HOCu-Z). A low intensity band at 10,000–15,000 cm^{-1} was previously assigned to the d–d transition characteristic of d [9] Cu^{2+} [26]. This band was at a lower frequency than calculated for the 8-MR ring of the Z-CuOH.HOCu-Z species (10,000–20,000 cm^{-1}). The spectral resolution did not allow observation of the presence of smaller amounts of other species such as oxide clusters of the types Z-Cu_3O_3-Z and Z-Cu-O-Cu-Z, formed by hydrolysis reaction of compensating Cu^{2+} cations, with the formation of primary Z-CuOH species, during thermal treatment in O_2 [26,27] or CO_2. Interestingly, similar spectra were obtained for treatment using O_2 or CO_2, with the results suggesting that the predominant species (Z-CuOH.HOCu-Z) did not undergo either dehydration to Z-Cu-O-Cu-Z or autoreduction to Z-Cu^+. Hence, in the chemical looping process using Cu-MAZ, the heat treatment after the step of methanol extraction by H_2O vapor did not need to be performed in an O_2 atmosphere.

Based on the assumption that the species reoxidized by CO_2 would also undergo autoreduction in Ar, the 2Cu2.7MAZ sample (5.5 wt% Cu) was subjected to thermal treatments in different atmospheres (O_2, CO_2, and Ar). Figs. 4(a), 4(b), and 4(d) show the subtraction of the spectra for the 2Cu2.7MAZ sample initially heated in O_2 at 450 ºC for 1 h, followed by treatment in Ar at 450 ºC for 1 h, and finally treatment in CO_2 for 1 h. The subtraction of the spectra for the samples treated at 450 ºC in different atmospheres were denoted O_2-Ar and CO_2-Ar. Fig. 4(c) shows

$$2\ [Cu^{II}OH]^{+} \xrightarrow[-H_2O]{} [Cu^{II}\text{-}O\text{-}Cu^{II}]^{2+} \xrightarrow[-0.5O_2]{} [Cu^{I}\text{-}\square\text{-}Cu^{I}]^{2+}$$

Scheme 1. Pathway for copper autoreduction in MFI, MOR, and FAU zeolites [8].

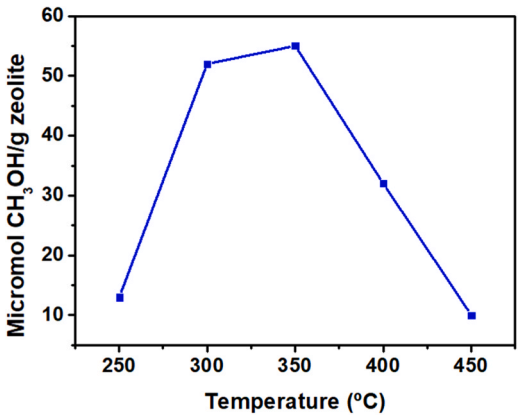

Fig. 1. Results obtained using the 1Cu2.7MAZ catalyst (3.2 wt% Cu) in isothermal processes, with CO_2 used for activation.

the subtraction of the spectra for the sample treated in CO_2 and then exposed to CH_4 (CO_2-CH_4). Fig. 4(a) shows the subtraction of the spectrum for species that were autoreduced in Ar, at 450 °C, from the spectrum for the sample treated in O_2. Fig. 4(b) shows that the same species autoreduced in Ar were reoxidized in the thermal treatment with CO_2. These spectra contained low intensity bands at around 30,000–32,000 cm^{-1}, together with an intense band at around 38,000 cm^{-1}.

The results indicated the following: I) The sample treated in O_2 was autoreduced in Ar (Fig. 4(a)); II) This autoreduced sample was re-oxidized in CO_2 (Fig. 4(b)); III) The presence of the species autoreduced in Ar (Fig. 4(a)) was not resolved in the UV-Vis spectra and also did not correspond to the predominant Z-CuOH.HOCu-Z species in the initial sample (shown in Fig. 3). The bands for these autoreduced species, which may have been present at low concentrations, were hidden by the bands of the Z-CuOH.HOCu-Z species; IV) It was also evident that this spectrum could not be resolved by comparison with the spectra calculated by DFT for the Z-Cu_2O_3-Z and Z-Cu-O-Cu-Z species (shown in Fig. 2). Based on these considerations, these bands could reasonably be attributed to the presence of anchored clusters of Z_n-Cu_xO_y type oxides that balanced the charges of the MAZ zeolite structure.

For the 2Cu2.7MAZ sample treated in CO_2 and used in the reaction with CH_4 at 450 °C, subtraction of the spectrum obtained in CO_2 from the spectrum in CH_4 resulted in the spectrum for the copper clusters that reacted with CH_4 (Fig. 4(c)). This spectrum was much more intense than when the sample was autoreduced with Ar. The main bands were at 36,000 and 43,000 cm^{-1}, in accordance with the spectra calculated by DFT (Fig. 2), corresponding to the Z-CuOH.HOCu-Z type species [11,26,27,29]. Therefore, this indicated that Z-CuOH.HOCu-Z was the main species in Cu-MAZ that reacted with CH_4. The spectra in Fig. 4(d) makes it evident that the self-reduced species in Ar is oxidized by both oxidants O_2 or CO_2. It is reasonable to suppose that the species autoreduced with Ar would also be reduced by CH_4, with its spectrum being enveloped by the bands of the main Z-CuOH.HOCu-Z species. For direct observation of the presence of Cu_xO_y type species, new experiments were performed, as described below.

In an attempt to identify all the species reduced by CH_4, *in situ* DRS UV-Vis analyses were performed with initial activation of the sample using O_2 or CO_2, at 450 °C, followed by cooling to 50 °C. During the temperature decrease, a spectrum was collected at 250 °C, for use as a background. The samples were then treated at 250 °C under a flow of CH_4. Hence, the background spectrum obtained in CO_2 or O_2 corresponded to the spectrum for all the Cu^{2+} species present in the sample. Subtraction of the background spectrum from the spectrum after treatment in CH_4, both at 250 °C, resulted in the spectrum for the species reduced by CH_4 in the first reaction cycle. The spectra resulting from the O_2-CH_4 and CO_2-CH_4 subtractions are shown in Figs. 5(a) and 5(b), respectively. The O_2-CH_4 spectrum showed charge transfer bands (Cu^{2+}→O) at around 36,000 and 41,300 cm^{-1}, corresponding to the main bands calculated by DFT for the Z-CuOH.HOCu-Z species (Fig. 2 (a)) formed during the thermal treatment of Cu-MAZ, when hydrated Cu^{2+} was hydrolyzed to Z-CuOH. Due to their proximity and the structure of the MAZ zeolite, these species were stabilized in the form of paired copper monomers, here denoted Z-CuOH.HOCu-Z [11,26,27,29]. The CO_2-CH_4 spectrum presented bands at 36,000, 39,500, and 42,

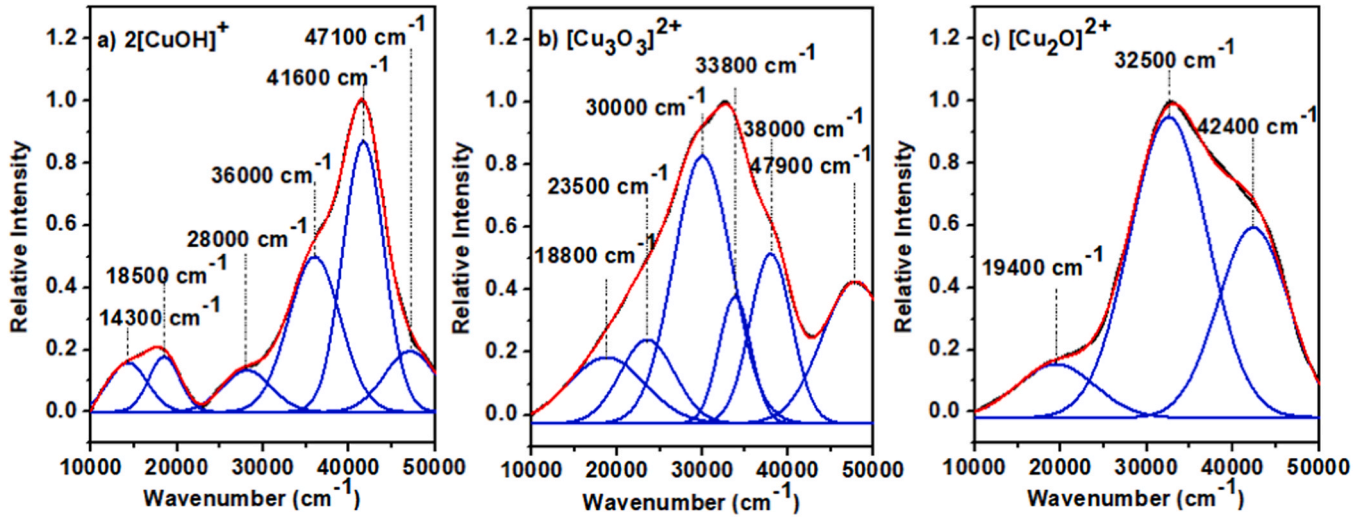

Fig. 2. Calculated UV-Vis spectra obtained using DFT for clusters of Cu species in 8-member rings (8-MR) of zeolite omega Cu-MAZ: (a) adjacent $2(CuOH)^{2+}$ species; (b) $[Cu_2O_3]^{2+}$ species; (c) $[Cu\text{-}O\text{-}Cu]^{2+}$ species.

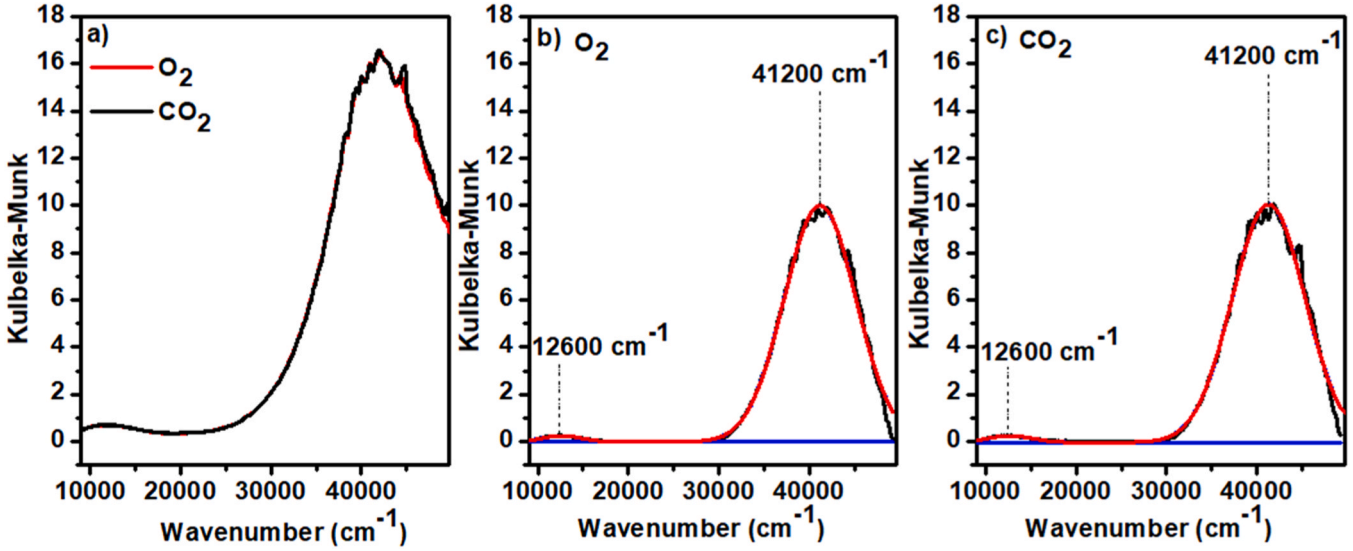

Fig. 3. DRS-UV-Vis spectra for the 2Cu2.7MAZ sample (5.5 wt% Cu): (a) Spectra during activation with O_2 or CO_2 at 450 ºC; (b) Species formed in the activation using O_2 at 450 ºC; (c) Species present after heating the sample under a flow of CO_2 at 450 ºC.

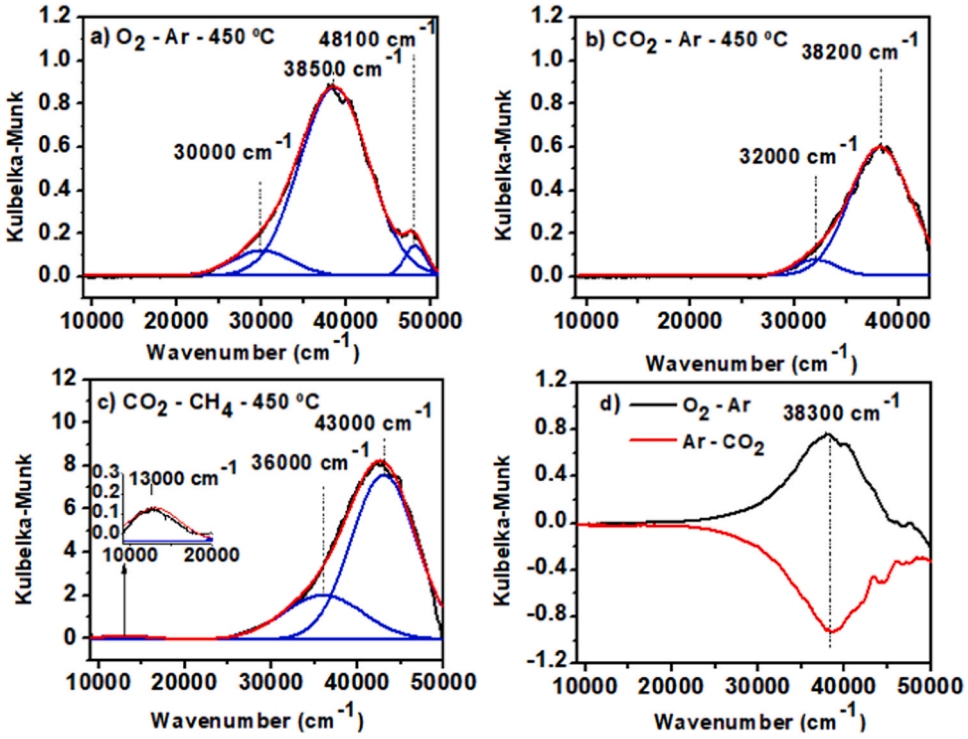

Fig. 4. DRS-UV-Vis spectra for the 2Cu2.7MAZ (5.5 wt% Cu) samples at 450 ºC: (a) Subtraction of the spectrum obtained under a flow of O_2 from the spectrum obtained under a flow of Ar; (b) Subtraction of the spectrum obtained under a flow of CO_2 from the spectrum obtained under a flow of Ar; (c) Subtraction of the spectrum obtained under a flow of CO_2 from the spectrum obtained under a flow of CH_4; (d) Subtraction of the spectrum obtained under a flow of O_2 from the spectrum obtained under a flow of Ar, and subtraction of the spectrum obtained under a flow of Ar from the spectrum obtained under a flow of CO_2, at 450 ºC.

100 cm^{-1}. The CO_2-CH_4 spectrum was generally indicative of high reflectance surfaces, compared to the sample only treated using O_2. The band assigned to the d–d transition characteristic of d [9] in the spectrum of the sample treated using CO_2 (Figs. 5(b) and 5(c)) presented low frequency splitting at 12,000 and 18,200 cm^{-1}, which was not present for the sample treated using O_2 (Fig. 5(a)). This was suggestive of the presence of more than one Cu^{2+} species that was reduced with methane after pretreatment using CO_2. The high intensity of the band at 39, 500 cm^{-1} suggested a contribution of Z-Cu_xO_y-Z species, with the spectrum being similar to that for the sample autoreduced in Ar (Fig. 4 (a)). The lower intensity of the band at 36,000 cm^{-1} for the sample treated using CO_2 suggested the presence of smaller amounts of Z-CuOH. HOCu-Z species, relative to Z-Cu_xO_y-Z species.

After reaction with CH_4 and extraction using H_2O vapor, the sample was reactivated in CO_2 at 450 ºC, cooled to 250 ºC in CO_2, and the spectrum obtained was denoted "CO_2-background-2nd cycle". After activation, this sample was placed in a flow of CH_4, at 250 ºC. Subtraction of the "CO_2-background-2nd cycle" spectrum from that for the

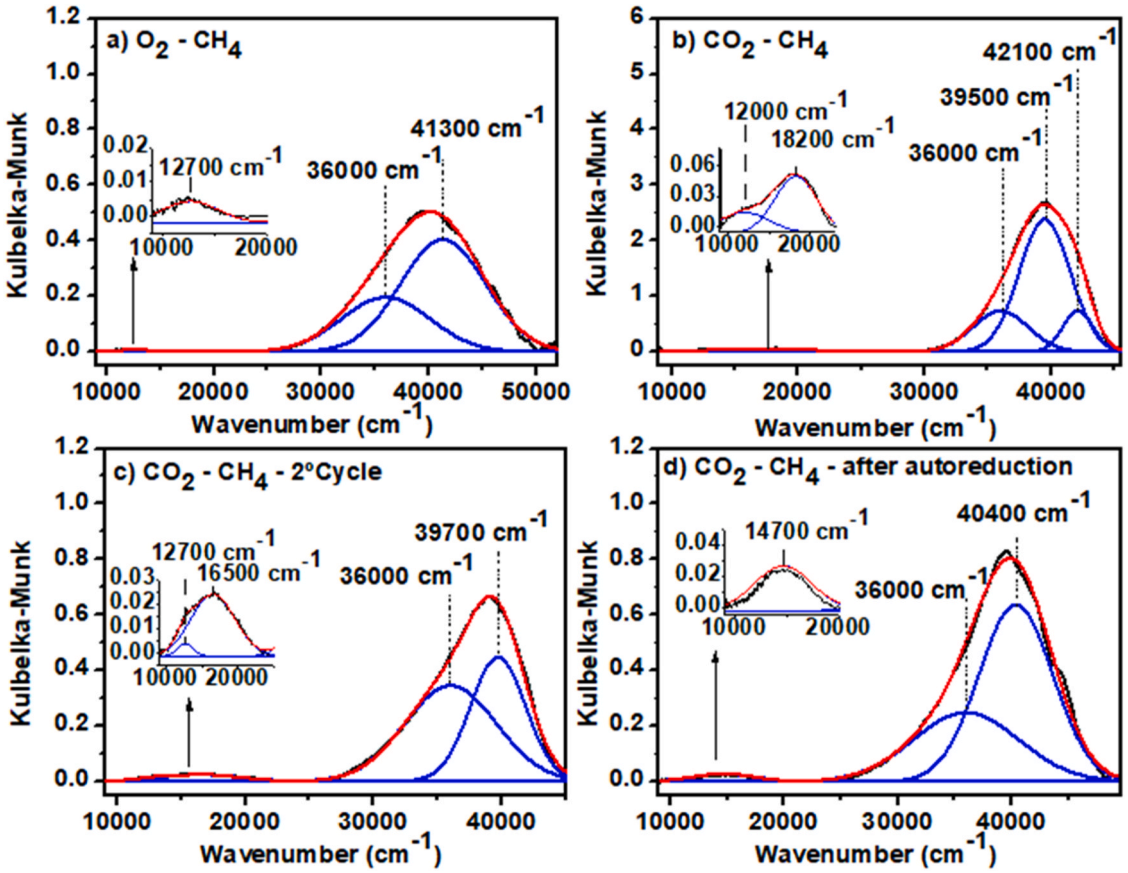

Fig. 5. Spectra resulting from subtraction of the spectrum acquired under a flow of oxidizing gas from the spectrum acquired under a flow of CH_4 for the sample with 5.5 wt% Cu, at 250 °C: (a) activation with O_2; (b) activation with CO_2; (c) reactivation with CO_2 (one reaction cycle with the sample was performed prior to the UV-Vis analysis); (d) reoxidation with CO_2 (with previous autoreduction of the sample).

sample in CH_4 resulted in the spectrum shown in Fig. 5(c). This spectrum presented bands at 36,000 and 39,700 cm^{-1}, with a high contribution of the species corresponding to the band at 36,000 cm^{-1}, and had a profile similar to that for species of the type Z-CuOH.HOCu-Z. However, comparison of the spectra for the species treated with CO_2 after the reactions in the first and second cycles (Figs. 5(b) and 5(c), respectively) showed that there was a small shift from 42,100 to 39,700 cm^{-1}, as well as a significant decrease in spectrum intensity between the first and second cycles. These features suggested that the species formed after extraction with H_2O vapor, followed by treatment with CO_2 in the second cycle, were of the types Z-CuOH.HOCu-Z.

Another analysis was performed with this sample after autoreduction in Ar at 450 °C and reoxidation in CO_2 at 450 °C. The spectrum obtained was denoted "CO_2-background-2nd cycle-Ar". The sample was then exposed to CH_4, at 250 °C. Subtraction of the "CO_2-background-2nd cycle-Ar" spectrum from the spectrum for the sample exposed to CH_4 is shown in Fig. 5(d). There was a small shift of the charge transfer band (O→Cu^{2+}) from around 39,700–40,400 cm^{-1}, although the profiles were very similar, in contrast to the spectrum for the sample in the first cycle that was not subjected to extraction using H_2O vapor (Fig. 5(b)). This indicated that species of the Z-Cu$_x$O$_y$-Z type were removed by autoreduction during treatment in Ar. Finally, a band at around 14,700 cm^{-1} (Fig. 5(d)) was characteristic of the Cu^{2+} cation d-d transition of the Z-CuOH.HOCu-Z species, as observed in the simulated spectra (Fig. 2) [30]. The number and position of bands at low frequency varied according to the heat treatment employed (Fig. 5), reflecting changes in Cu^{2+} coordination symmetry.

These results indicated that when the sample was initially activated in CO_2, there was the formation of a mixture of oxide species of the types Z-Cu$_x$O$_y$-Z and paired Z-CuOH monomers (Z-CuOH.HOCu-Z), with the latter being the main species present. As previously demonstrated by Sushkevich et al. [5], extraction with H_2O vapor promoted Cu$^+$ reoxidation, with formation of copper hydroxides. The spectrum shown in Fig. 5(c) suggested that the contribution of Z-Cu$_x$O$_y$-Z species became smaller than in the first cycle, before the extraction with H_2O vapor (Fig. 5(b)), indicating that treatment of the sample with H_2O vapor, followed by the CO_2 treatment, promoted the hydroxylation of Z-Cu$_x$O$_y$-Z oxides to form paired CuOH$^+$ monomers. It was also observed that under a flow of CH_4, the reduced species presented characteristic charge transfer bands (O→Cu^{2+}) that were similar with or without pre-reduction, as shown in the corresponding spectra (Figs. 5(d) and 5(b), respectively).

Table 4 shows activity data for samples with different Cu contents, activated using CO_2, with or without previous autoreduction. These treatments corresponded to those for the samples with the spectra shown in Figs. 5(d) and 5(b), respectively. For the 1Cu2.7MAZ sample with lower Cu content (3.2 wt% Cu), autoreduction led to lower activity,

Table 4
Comparison of catalytic tests using Cu2.7MAZ catalysts either previously autoreduced and reactivated with CO_2, or only activated with CO_2, without undergoing autoreduction.

Run	Catalyst	Previous catalyst autoreduction		No previous catalyst autoreduction	
		Micromol CH_3OH/g zeolite	Mol CH_3OH/mol Cu	Micromol CH_3OH/g zeolite	Mol CH_3OH/mol Cu
2	1Cu2.7MAZ	43	0.087	94	0.190
4	2Cu2.7MAZ	94	0.109	111	0.127

compared to the sample that was not autoreduced. For the 2Cu2.7MAZ sample with higher Cu content (5.5 wt% Cu), the effect of autoreduction on activity was within the experimental error. These results indicated that polynuclear oxide species of the type Z_n-$Cu_{(x>3)}O_y$, which were autoreduced in Ar, were formed from the hydrolyzed $[CuOH]^{2+}$ species, since the low concentration of Cu^{2+} ions was unfavorable for formation of paired copper monomers of the type Z-CuOH.HOCu-Z. It was proposed previously that when Cu-MOR was autoreduced, the $[CuOH]^{2+}$ species in the cavities migrated to form Z_2-Cu_3O_3 oxide species [28]. Hence, the present results indicated that polynuclear species of the type Z_n-$Cu_{(x>3)}O_y$ were autoreduced in Ar at 450 ºC and were reoxidized by CO_2, as shown by the results in Fig. 4.

The Z_n-$Cu_{(x>3)}O_y$ and Z-CuOH.HOCu-Z species were present in the 1Cu2.7MAZ sample activated using CO_2, where the Z_n-$Cu_{(x>3)}O_y$ species had a greater contribution to the catalytic activity (Table 4). The tests shown in Table 5 were performed in an attempt to determine the contributions of these species to the activity in the direct oxidation of CH_4 to methanol at 250 ºC. Firstly, the sample activated in CO_2 (at 450 ºC) was exposed to CH_4 (at 250 ºC), resulting in the formation of 92 μmol CH_3OH/g zeolite (Table 5, run 9). For the sample activated in CO_2 (at 450 ºC), exposed to CH_4 (at 250 ºC), and then heated in CO_2 (at 450 ºC), there was formation of only 6 μmol CH_3OH/g zeolite (Table 5, run 10). These tests indicated that the methanol formed was desorbed and oxidized when the sample was treated at 450 ºC in CO_2. Hence, it appeared that exposure of the active Z_n-$Cu_{(x>3)}O_y$ and Z-CuOH.HOCu-Z species to CH_4 at 250 ºC led to their reduction to Cu^+. In the next step, this sample was reoxidized at 450 ºC with CO_2 and was again exposed to CH_4 (at 250 ºC). The results (Table 5, run 11) indicated formation of 24 μmol CH_3OH/g zeolite.

Initially, the Z_n-$Cu_{(x>3)}O_y$ and Z-CuOH.HOCu-Z active species were responsible for the formation of 92 μmol CH_3OH/g zeolite (Table 5, run 9), while when the species reduced by CH_4 were reoxidized by CO_2, there was only reoxidation of the Z_n-$Cu_{(x>3)}O_y$ species, which were responsible for the formation of 24 μmol CH_3OH/g zeolite, corresponding to 26% of the total activity. These findings indicated that methanol could be desorbed with CO_2, without over-oxidation of methanol, using Cu-MAZ containing only the Z-CuOH.HOCu-Z active species, where the Cu^+ formed in the oxidation of CH_4 was not reoxidized with CO_2.

Fig. 6(a) shows the spectrum of the sample activated in O_2, corresponding to the active species that were reduced by CH_4 after 60 min at 350 ºC, with bands at 36,300 and 42,100 cm^{-1}. Comparison of the spectra in Figs. 5(a) and 6(a) corresponding to the 2Cu2.7MAZ sample activated in O_2 and reacted with CH_4 at 250 and 350 ºC, respectively, showed that they were similar and reflected the presence of Z-CuOH.HOCu-Z species. However, the spectra acquired at 350 ºC showed greater intensity of the bands and a small shift towards higher frequency, compared to the spectra acquired at 250 ºC. These results indicated the reduction of a greater quantity of active species at 350 ºC. However, the shift towards higher frequency, as reported by Li et al. [27], reflected variation of the Cu-O bond distance, as well as lower reactivity with CH_4.

The spectrum shown in Fig. 6(b) corresponds to the species reoxidized by CO_2 after one reaction cycle, with bands at around 38,100 and 43,000 cm^{-1} attributed to oxide species (Z_n-Cu_xO_y). Fig. 6(c) shows the species that reacted with CH_4 in a second reaction cycle. From the first to the second reaction cycle, the bands shifted from 36,300 and 42,100 cm^{-1} to 36,000 and 41,100 cm^{-1}. The intensities of these bands decreased substantially, indicating a much smaller fraction of active sites in the second cycle, since reoxidation with CO_2 only reactivated Z_n-Cu_xO_y oxide sites, without reoxidation of the main active species (Z-CuOH.HOCu-Z).

Interestingly, when the samples activated using O_2 or CO_2 were exposed to CH_4 at 350 ºC, the spectra showed an active species band at around 13,000 cm^{-1}, assigned to the d–d transition feature characteristic of d [9] of Cu^{2+} [26]. On the other hand, when the sample activated using CO_2 was exposed to CH_4 at 250 ºC, there was band splitting between 12,000 and 18,000 cm^{-1}, indicating that the symmetry of the Cu^{2+} ions changed according to their reactivity.

3.1. CO_2 Activation over $MAZ[Cu_2^+]^{2+}$

To re-oxidize the Cu^+ to Cu^{2+} activated with CO_2, the process involves two stages: the first consist in the adsorpion of CO_2 in the $MAZ[Cu_2^I]^{2+}$ and the second, the direct dissociation of the CO_2 *via* a redox process in which the $[Cu^{2+} - O_1 - Cu^{2+}]^{2+}$ species is formed, and subsequently, this could promote the regeneration of Z-CuOH…HOCu-Z active species, in the presence of a H_2O molecule. Using DFT periodic calculations with the PBE-D3 functional we evaluated the CO_2 adsorption and activation by $MAZ[Cu_2^+]^{2+}$. Model systems and Theoretical methods are detailed in Supporting Material.

The CO_2 adsorption process on active site occur *via* the interaction of CO_2 with the two Cu^+ sites through of the C − O_1 bond. Due to the spatial arrangement of the Cu^+ cations, the CO_2 molecule is not located centrally in the middle of the adsorption site, therefore, Cu_1 − O_1 and Cu_2 − O_1 electrostatic interaction distances differ (2.351 and 2.552 Å, respectively), as well as the angles formed by Cu_1 − O_1 − C and Cu_2 − O_1 − C atoms which amount to 139° and 156°, respectively. In this stage, the O_1 − CO bond is elongated from original value of 1.120–1.282 Å (see Fig. 7), while the angle in CO_2 molecule is slightly bent from 180° to 173°. These results are in agreement with the results reported in the literature for the adsorption of CO_2 in MFI-Cu^+ [31].

The CO_2 binding is exothermic by − 52 kJ mol^{-1} and a CO_2 adsorbs with an E_{ads}= − 15.753 kJmol^{-1}. Low adsorption strength may be explained as a result of the steric effect exerted by the framework of the nanopore of MAZ zeolite, which also is evidenced for the variation in the CO_2 angle during the adsorption process [32]. and the CO_2 is allocated close of the wall zeolite. Our theoretical calculation predicts than for active site formation to occur, the direct dissociation of O_1 − CO bond must go through a transition state that requires E_a= 142 kJ mol^{-1} to reach. TS structure show that the dissociation O_1 − CO distance is of 1.456 Å, while the angle in CO_2 molecule is 20° less that in RC structure, regarding the active site the Cu_1 − O and Cu_2 − O bonds become symmetric with a value of 1.977 Å and a $[Cu_1 - O_1 - Cu_2]^{\neq}$ angle of 74°, . In the transition state, the Van der Waals interaction at distances less 3.100 Å between the CO_2 molecule with the O atoms of the 4 − MR opposite the $[Cu_1 - O_1 - Cu_2]^{2+}$ site, play an important role slightly disrupting the framework structure, and charge fluctuations that result in a nonspecific, nondirectional attraction, in addition a short interaction between O_i −O_1 at 2.312 Å, is observed (see Fig. 7). Later of this step, the reaction product is slightly stabilized and E_{rxn} = − 10, 253 kJ mol^{-1}. Thus, due to the weak interaction between Cu^{+1} cations with the CO_2 molecule and the strong interaction of CO_2 with the zeolite

Table 5
Reactions using the 1Cu2.7MAZ catalyst with methanol desorption using CO_2 at 450 ºC.

Run	Oxidant gas	1st activation at 450 ºC (min)	1st reaction at 250 ºC (min)	2nd activation / desorption of CH_3OH at 450 ºC (min)	2nd reaction at 250 ºC (min)	Micromol CH_3OH/g zeolite	Mol CH_3OH/ mol Cu
9	**CO_2**	60	30	-	-	92	0.186
10	**CO_2**	60	30	60	-	6	0.013
11	**CO_2**	60	30	60	30	24	0.049

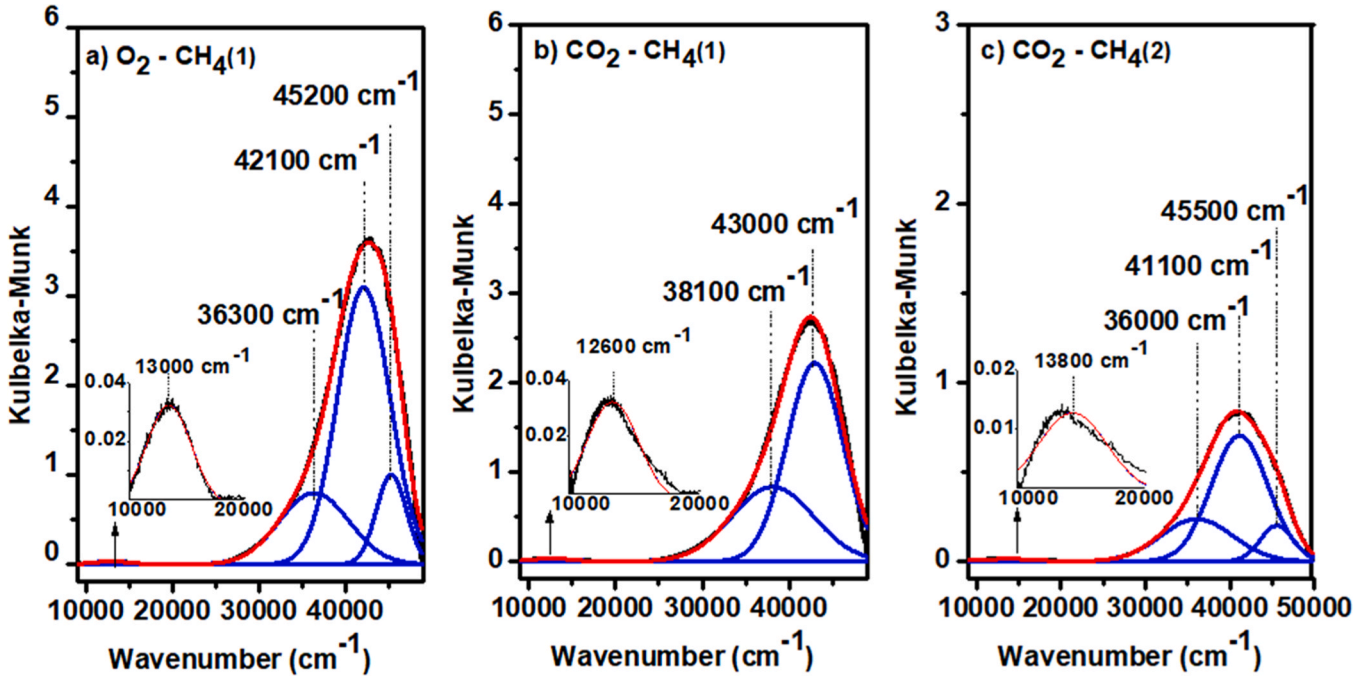

Fig. 6. Spectra for the 2Cu2.7MAZ (5.5 wt% Cu) sample resulting from subtraction of the spectrum acquired under a flow of oxidizing gas from the spectrum acquired under a flow of CH_4 at 350 °C: (a) subtraction of the spectrum acquired at the end of activation with O_2 from the spectrum acquired in the first step with CH_4; (b) subtraction of the spectrum acquired at the end of reoxidation with CO_2 from the spectrum acquired at the end of reduction with CH_4 (first step with CH_4); (c) subtraction of the spectrum acquired at the end of reoxidation with CO_2 from the spectrum acquired in the second step with CH_4.

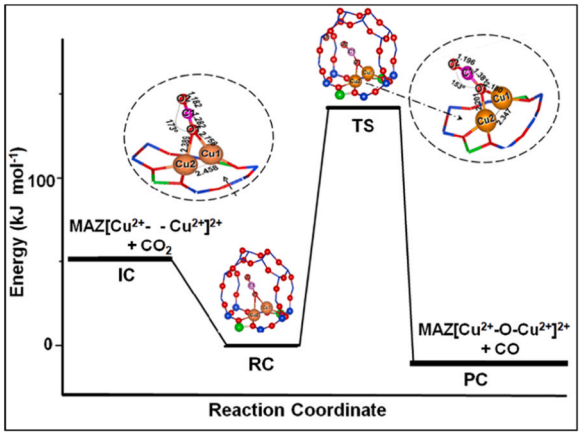

Fig. 7. Computed energy diagram for CO_2 activation over $MAZ[Cu_2^I]^{2+}$ site, **IC**, **RC**, **TS**, and **PC** are initial complex, reactant complex, transition state, and product complex, respectively. Only the active sites and zeolite pore are shown, while the other atoms of the zeolite are omitted for clarity. Color code: blue (Si), red (O), green (Al), orange (Cu), and magenta (C).

wall, nondirectional charge fluctuations prevent the CO_2 activation.

4. Discussion

In catalysts derived from Cu^{2+}-exchanged zeolites and subjected to heat treatment in Ar at high temperature (450 °C), it is well known that the Cu^{2+} ions compensating the charge of the zeolite structure can undergo hydrolysis reactions to form active species with structures such as Z-Cu-O-Cu-Z, Z-Cu_3O_3-Z, and Z-CuOH.HOCu-Z. [3,5,8–10] In a study of Cu-exchanged MOR, MFI, BEA, and FAU zeolites, Sushkevich et al. [8] found that the zeolite topology and Si/Al ratio significantly influenced the onset temperature and rate of copper reduction of the active species formed. These results showed the need for heat treatment in an oxidizing gas such as O_2 [33].

The results obtained in the present work showed that O_2 could be replaced by CO_2 in the initial treatment of Cu^{2+}-exchanged MAZ. Irrespective of the atmosphere used in the heat treatment (CO_2 or O_2), the main structures formed in MAZ were paired copper monomers of the type Z-CuOH.HOCu-Z, as observed previously using O_2 [11]. The Z_n-$Cu_{(x>3)}O_y$ type oxide structure was present in smaller amounts. The type of structure Cu-O cluster formed was strongly dependent on the Cu/Al ratio, with formation of Z_n-$Cu_{(x>3)}O_y$ being favored at low ratios. The Z_n-$Cu_{(x>3)}O_y$ oxide species was autoreducible in Ar at 450 °C, consequently requiring the presence of an oxidant such as O_2 to maintain the oxide in the Cu^{2+} form during heat treatment. The results demonstrated that CO_2 could be used instead of O_2 to protect oxide species such as $Cu_{(x>3)}O_y$ during treatment at high temperature (450 °C). In contrast, the Z-CuOH.HOCu-Z species was highly stable at 450 °C and did not require the presence of any oxidant. The species in the structure of MAZ have inherently high thermal stability. Therefore, CO_2 can be used instead of O_2 in heat treatment using the chemical looping process, representing an advance in terms of process safety, considering explosion risks and ease of operation. Pressure has been reported to have a positive effect on the methanol yield for CH_4 oxidation [9,13]. At 250 °C and pressure of 1 atm, reduction of the total Cu^{2+} ions was low, at around 26% (Table 1). A higher reaction temperature significantly increased reaction of the active Z-CuOH.HOCu-Z species in the MAZ, which was accompanied by a shift of the UV-Vis bands to higher frequency, indicating that more stable species started to react with CH_4 at higher temperature (350 °C). Increased conversion by the active species could not be attributed only to greater accessibility for CH_4. Small modifications in the structure resulted in a distribution of reactivity of the active Z-CuOH.HOCu-Z species with CH_4, requiring reaction temperatures above 250 °C for high conversion. Although pressure has been reported to have a positive effect on methanol yield, the effect of temperature appears to be crucial for increasing the conversion. However, a higher temperature may favor the desorption and oxidation of methanol. It is well known that in the chemical looping process, methane is oxidized by Cu^{2+} clusters in zeolites, forming methanol and Cu^{+}, at

temperatures of around 250 ºC [6]. Reoxidation of Cu^{+} occurs in the step of methanol desorption with water vapor [5]. Due to the structure of the MAZ zeolite, the Cu^{+} species formed from Z-CuOH.HOCu-Z do not activate the CO_2 molecule and the Cu^{+} is not reoxidized. According to DFT calculation, due to the weak interaction between Cu^{+1} cations with the CO_2 and the strong interaction of CO_2 with the zeolite, nondirectional charge fluctuations prevent the CO_2 activation. Thus, for active specie Z-CuOH.HOCu-Z it is not possible to replace water by CO_2 in the methanol desorption step. Nevertheless, the Cu^{+} formed from $Cu_{(x>3)}O_y$ species is oxidized by CO_2, opening a new opportunity for the development of Cu-zeolite for use in the chemical looping process at high temperature, replacing O_2 by CO_2, after the step of methanol desorption with H_2O vapor.

5. Conclusions

This work reports a new process for the conversion of methane to methanol, where O_2 is replaced by CO_2 in the step for reactivation of the Cu-MAZ catalyst.

Subtraction of the *in situ* DRS UV-Vis spectra obtained for different reactants enabled the spectra fraction of the active species to be obtained at region in high frequencies characteristic of charge transfer bands (Cu^{2+}→O). The active species present in Cu-MAZ were paired copper monohydroxide monomers (Z-CuOH.HOCu-Z) and polyoxides of the type Z_n-$Cu_{(x>3)}O_y$. The type of structure was strongly dependent on the Cu/Al ratio, with formation of the Z_n-$Cu_{(x>3)}O_y$ type structure being favored at a low Cu/Al ratio.

The Z_n-$Cu_{(x>3)}O_y$ and Z-CuOH.HOCu-Z species in Cu-MAZ showed high activity for CH_4 oxidation at temperature above 250 ºC, with reduction of between 24% and 38% of the total Cu contained in Cu-MAZ.

After reduction with CH_4, the Z_n-$Cu_{(x>3)}O_y$ species could be reoxidized with CO_2, while the Z-CuOH.HOCu-Z species could not be reoxidized with CO_2, but could be reoxidized in the presence of water vapor.

The Z_n-$Cu_{(x>3)}O_y$ species was protected against autoreduction when heated in CO_2 at 450 ºC, while the Z-CuOH.HOCu-Z type structure in Cu-MAZ was highly thermally stable in CO_2 at 450 ºC. Hence, CO_2 could be used instead of O_2 in the step for reactivation of the active species in Cu-MAZ, after extraction of methanol with water vapor. The use of CO_2 allows safe and fast dynamic modulation of the CH_4, H_2O, and CO_2 reactants in the reactor feed, in a chemical looping process.

CRediT authorship contribution statement

Tássia Caroline. P. Pereira, Jussara V. R. Vieira: Conceptualization, Methodology, Investigation, Data curation, Writing – original draft. **Carlos H. F. da Cunha, Ana C. M. Tello, Alice M. de Lima, Asdrubal L. Blanco, Alejandro Lopez-Castillo:** Methodology and Softwares utilized for DFT calculations. Stefanie C. M. Mizuno, Yasmin O. Carvalho, Thiago Faheina, Monize Picinini, Ernesto A. Urquieta-Gonzalez, João Batista O. dos Santos: Contributed equally in Conceptualization and Experimental supports. **José Maria Correa Bueno:** Project administration, Funding acquisition, Supervision, Writing – review & editing.

Declaration of Competing Interest

The authors declare that they have no known competing financial interests or personal relationships that could have appeared to influence the work reported in this paper.

Data Availability

No data was used for the research described in the article.

Acknowledgements

This work was supported by the São Paulo State Research Foundation (FAPESP, grants 2018/26459–3, 2018/01258–5, and 2019/12501–0) and the National Council for Scientific and Technological Development (CNPq, grant 132827/2018-2). This study was financed in part by the Coordenacão de Aperfeicoamento de Pessoal de Nível Superior, Brasil (CAPES, Finance Code 001). The authors also thank Ricardo Passini for assistance during the UV-Vis experiments.

The calculations performed here made use of the computational resources of the Center of Mathematical Sciences Applied to Industry (CeMEAI) funded by FAPESP (grant 2013/07375-0).

The authors also thank LCE-DEMa (UFSCar) for the Scanning Electron Microscopy (SEM) analyzis and the student **Gustavo Iga** of the Department of Chemistry at UFSCar for the Nuclear Magnetic Resonance Spectroscopy (NMR) analyzis.

Appendix A. Supporting information

Supplementary data associated with this article can be found in the online version at doi:10.1016/j.apcatb.2023.123370.

References

[1] A.I. Olivos-Suarez, À. Szécsényi, E.J.M. Hensen, J. Ruiz-Martinez, E.A. Pidko, J. Gascon, Strategies for the Direct catalytic valorization of methane using heterogeneous catalysis: challenges and opportunities, ACS Catal. 6 (5) (2016) 2965–2981, https://doi.org/10.1021/acscatal.6b00428.

[2] Z. Zakaria, S.K. Kamarudin, Direct conversion technologies of methane to methanol: an overview, Renew. Sustain. Energy Rev. 65 (2016) 250–261, https://doi.org/10.1016/J.RSER.2016.05.082.

[3] M. Ravi, M. Ranocchiari, J.A. van Bokhoven, The direct catalytic oxidation of methane to methanol—a critical assessment, Angew. Chem. - Int. Ed. 56 (52) (2017) 16464–16483, https://doi.org/10.1002/anie.201702550.

[4] E.I. Solomon, D.E. Heppner, E.M. Johnston, J.W. Ginsbach, J. Cirera, M. Qayyum, M.T. Kieber-Emmons, C.H. Kjaergaard, R.G. Hadt, L. Tian, Copper active sites in biology, Chem. Rev. 114 (7) (2014) 3659–3853, https://doi.org/10.1021/CR400327T.

[5] V.L. Sushkevich, D. Palagin, M. Ranocchiari, J.A. van Bokhoven, Selective anaerobic oxidation of methane enables direct synthesis of methanol, Science 356 (6337) (2017) 523–527, https://doi.org/10.1126/science.aam9035.

[6] V.L. Sushkevich, J.A. van Bokhoven, Kinetic study and effect of water on methane oxidation to methanol over copper-exchanged mordenite, Catal. Sci. Technol. 10 (2) (2020) 382–390, https://doi.org/10.1039/c9cy01711a.

[7] V.I. Sobolev, K.A. Dubkov, et al., Selective oxidation of methane to methanol on a FeZSM-5 surface, Catal. Today 24 (1995) 251–252.

[8] V.L. Sushkevich, A. v Smirnov, J.A. van Bokhoven, Autoreduction of copper in zeolites: role of topology, Si/Al ratio, and copper loading, J. Phys. Chem. C 123 (15) (2019) 9926–9934, https://doi.org/10.1021/acs.jpcc.9b00986.

[9] A.J. Knorpp, M.A. Newton, S.C.M. Mizuno, J. Zhu, H. Mebrate, A.B. Pinar, J.A. Van Bokhoven, Comparative performance of cu-zeolites in the isothermal conversion of methane to methanol, Chem. Commun. 55 (78) (2019) 11794–11797, https://doi.org/10.1039/c9cc05659a.

[10] A.J. Knorpp, A.B. Pinar, M.A. Newton, V.L. Sushkevich, J.A. van Bokhoven, M.A. Z. Copper-Exchanged Omega, Zeolite: copper-concentration dependent active sites and its unprecedented methane to methanol conversion, ChemCatChem 10 (24) (2018) 5593–5596, https://doi.org/10.1002/cctc.201801809.

[11] A.J. Knorpp, A.B. Pinar, C. Baerlocher, L.B. McCusker, N. Casati, M.A. Newton, S. Checchia, J. Meyet, D. Palagin, J.A. van Bokhoven, Paired Copper monomers in zeolite omega: the active site for methane-to-methanol conversion, Angew. Chem. - Int. Ed. 60 (11) (2021) 5854–5858, https://doi.org/10.1002/anie.202014030.

[12] J.P. Lange, V.L. Sushkevich, A.J. Knorpp, J.A. van Bokhoven, Methane-to-methanol via chemical looping: economic potential and guidance for future research, Ind. Eng. Chem. Res (2019), https://doi.org/10.1021/acs.iecr.9b01407.

[13] A.J. Knorpp, M.A. Newton, V.L. Sushkevich, P.P. Zimmermann, A.B. Pinar, J.A. van Bokhoven, The influence of zeolite morphology on the conversion of methane to methanol on copper-exchanged omega zeolite (MAZ), Catal. Sci. Technol. 9 (11) (2019) 2806–2811, https://doi.org/10.1039/c9cy00013e.

[14] M. Hurme, M. Rahman, Implementing inherent safety throughout process lifecycle, J. Loss Prev. Process Ind. 18 (4–6) (2005) 238–244, https://doi.org/10.1016/J.JLP.2005.06.013.

[15] W. Pu, A.A. Abdul Raman, M.D. Hamid, X. Gao, A. Buthiyappan, Inherent safety concept based proactive risk reduction strategies: a review, J. Loss Prev. Process Ind. 84 (2023), 105133, https://doi.org/10.1016/J.JLP.2023.105133.

[16] Y. Gambo, S. Adamu, G. Tanimu, I.M. Abdullahi, R.A. Lucky, M.S. Ba-Shammakh, M.M. Hossain, CO_2-mediated oxidative dehydrogenation of light alkanes to olefins: advances and perspectives in catalyst design and process improvement, Appl. Catal. A Gen. 623 (2021), 118273, https://doi.org/10.1016/J.APCATA.2021.118273.

[17] S.T. Rahman, J.R. Choi, J.H. Lee, S.J. Park, The role of CO_2 as a mild oxidant in oxidation and dehydrogenation over catalysts: a review, *2020, Vol. 10, Page 1075*, Catalysts 10 (9) (2020) 1075, https://doi.org/10.3390/CATAL10091075.
[18] P. Massiani, F. Fajula, F. Figueras, J. Sanz, 29Si and 27Al MAS n.m.r. Study of the distribution of Si and Al atoms in various forms of synthetic zeolite omega, Zeolites 8 (4) (1988) 332–337, https://doi.org/10.1016/S0144-2449(88)80132-5.
[19] A.M. Goossens, E.J.P. Feijen, G. Verhoeven, B.H. Wouters, P.J. Grobet, P.A. Jacobs, J.A. Martens, Crystallization of MAZ-type zeolites using tetramethylammonium, sodium and n-hexane derivatives as structure- and composition-directing agents, Microporous Mesoporous Mater. 35–36 (2000) 555–572, https://doi.org/10.1016/S1387-1811(99)00250-4.
[20] A. Ogawa, K. Iyoki, Y. Kamimura, S.P. Elangovan, K. Itabashi, T. Okubo, Seed-directed, rapid synthesis of MAZ-type zeolites without using organic structure-directing agent, Microporous Mesoporous Mater. 186 (2014) 21–28, https://doi.org/10.1016/J.MICROMESO.2013.11.026.
[21] M.A. Newton, A.J. Knorpp, A.B. Pinar, V.L. Sushkevich, D. Palagin, J.A. van Bokhoven, On the mechanism underlying the direct conversion of methane to methanol by copper hosted in zeolites; braiding Cu K-edge XANES and reactivity studies, J. Am. Chem. Soc. 140 (32) (2018) 10090–10093, https://doi.org/10.1021/jacs.8b05139.
[22] V.L. Sushkevich, R. Verel, J.A. Bokhoven, Pathways of methane transformation over copper-exchanged mordenite as revealed by insitu NMR and IR spectroscopy, Angew. Chem. Int. Ed. 59 (2) (2020) 910–918, https://doi.org/10.1002/anie.201912668.
[23] D. Palagin, V.L. Sushkevich, J.A. van Bokhoven, Water molecules facilitate hydrogen release in anaerobic oxidation of methane to methanol over Cu/mordenite, ACS Catal. 9 (11) (2019) 10365–10374, https://doi.org/10.1021/acscatal.9b02702.
[24] M.H. Groothaert, P.J. Smeets, B.F. Sels, P.A. Jacobs, R.A. Schoonheydt, Selective oxidation of methane by the Bis(μ-Oxo)dicopper core stabilized on ZSM-5 and mordenite zeolites, J. Am. Chem. Soc. 127 (5) (2005) 1394–1395, https://doi.org/10.1021/ja047158u.
[25] S. Grundner, M.A.C. Markovits, G. Li, M. Tromp, E.A. Pidko, E.J.M. Hensen, A. Jentys, M. Sanchez-Sanchez, J.A. Lercher, Single-site trinuclear copper oxygen clusters in mordenite for selective conversion of methane to methanol, Nat. Commun. 6 (1) (2015) 7546, https://doi.org/10.1038/ncomms8546.
[26] R. Oord, J.E. Schmidt, B.M. Weckhuysen, Methane-to-methanol conversion over zeolite Cu-SSZ-13, and its comparison with the selective catalytic reduction of NOx with NH3, Catal. Sci. Technol. 8 (4) (2018) 1028–1038, https://doi.org/10.1039/c7cy02461d.
[27] H. Li, C. Paolucci, I. Khurana, L.N. Wilcox, F. Göltl, J.D. Albarracin-Caballero, A. J. Shih, F.H. Ribeiro, R. Gounder, W.F. Schneider, Consequences of exchange-site heterogeneity and dynamics on the UV-visible spectrum of Cu-exchanged SSZ-13, Chem. Sci. 10 (8) (2019) 2373–2384, https://doi.org/10.1039/c8sc05056b.
[28] T. Ikuno, S. Grundner, A. Jentys, G. Li, E. Pidko, J. Fulton, M. Sanchez-Sanchez, J. A. Lercher, Formation of active Cu-Oxo clusters for methane oxidation in Cu-exchanged mordenite, J. Phys. Chem. C 123 (14) (2019) 8759–8769, https://doi.org/10.1021/acs.jpcc.8b10293.
[29] S.C.M. Mizuno, S. Dulnee, T.C.P. Pereira, R.J. Passini, E.A. Urquieta-Gonzalez, J.M. R. Gallo, J.B.O. Santos, J.M.C. Bueno, Stepwise methane to methanol conversion: effect of copper loading on the formation of active species in copper-exchanged mordenite, Catal. Today (2021), https://doi.org/10.1016/j.cattod.2020.11.027.
[30] C. Negri, M. Signorile, N.G. Porcaro, E. Borfecchia, G. Berlier, T.V.W. Janssens, S. Bordiga, Dynamic CuII/CuI speciation in Cu-CHA catalysts by in situ diffuse reflectance UV–Vis-NIR spectroscopy, Appl. Catal. A Gen. 578 (2019) 1–9, https://doi.org/10.1016/j.apcata.2019.03.018.
[31] G. Alonso, E. López, F. Huarte-Larrañaga, R. Sayós, H. Prats, P. Gamallo, Zeolite-encapsulated single-atom catalysts for efficient CO_2 conversion, J. CO_2 Util. 54 (2021), 101777, https://doi.org/10.1016/J.JCOU.2021.101777.
[32] M.H. Mahyuddin, A. Staykov, Y. Shiota, K. Yoshizawa, Direct conversion of methane to methanol by metal-exchanged ZSM-5 zeolite (Metal = Fe, Co, Ni, Cu), ACS Catal. 6 (12) (2016) 8321–8331, https://doi.org/10.1021/ACSCATAL.6B01721/ASSET/IMAGES/LARGE/CS-2016-017214_0007.JPEG.
[33] B. Michalkiewicz, Partial oxidation of methane to formaldehyde and methanol using molecular oxygen over Fe-ZSM-5, Appl. Catal. A Gen. 277 (1–2) (2004) 147–153, https://doi.org/10.1016/J.APCATA.2004.09.005.